A Study on the Performance Stability and the Water management of PEFC with Interdigitated Gas Flow Channels formed on a Gas Diffusion Layer

- Improvement of Performance Stability under high & low humidification conditions and clarification of the mechanisms by experimental and numerical analysis -

Tatsuya Inoue [1),2)] Daiki Sakai [1)] Kazuyuki Hirota [1)] Koichi Sano [1)] Naoki Hirayama [3)] Mitsunori Nasu [3)] Takahiro Suzuki [4)] Shouji Tsushima [4)] Junji Inukai [5)] Masahiro Watanabe [6)] Akihiro Iiyama [6)] Makoto Uchida [6)]

1) Suzuki Motor Corporation, Hamamatsu, 432-8611, Japan

E-mail: tatsuyainoue@hhq.suzuki.co.jp, daikisakai@hhq.suzuki.co.jp, kazuhirota@hhq.suzuki.co.jp, sanokoichi@hhq.suzuki.co.jp

2) Interdisciplinary Graduate School of Medicine and Engineering, University of Yamanashi, Kofu, 400-8511, Japan

3) Enomoto Co., Ltd., Uenohara-city, 409-0198, Japan

Hirayama-naoki@enomoto.co.jp, nasu-mitsunori@enomoto.co.jp

4) Osaka University, Suita, 565-0871, Japan

suzuki@mech.eng.osaka-u.ac.jp, tsushima@mech.eng.osaka-u.ac.jp

5) Clean Energy Research Center, University of Yamanashi, Kofu, 400-8510, Japan

jinukai@yamanashi.ac.jp

6) Hydrogen and Fuel Cell Nanomaterials Center, University of Yamanashi, Kofu 400-0021, Japan

m-watanabe@yamanashi.ac.jp, aiiyama@yamanashi.ac.jp, uchidam@yamanashi.co.jp

ABSTRACT: A new design concept for polymer electrolyte fuel cells that included a flat-metal separator and a gas diffusion layer (GDL) with interdigitated gas flow channels (FCs), was developed in our previous research. This new design cell of the interdigitated flow channel on the GDL with porous ribs has a clear advantage over the conventional design of interdigitated flow channel on the separator with solid ribs in being able to maintain higher performance under conditions of both water excess and water shortage. We suggested that these advantages are caused by the porous ribs which contribute to proper water management in the cell, as well to increase temperature around the GDL/MEA interface to avoid water accumulation. In this study, to validate the mechanism of the newly designed cell, the temperature distribution is analyzed by numerical simulation and the water distribution is analyzed by visualization technique by neutron radiography imaging. From these results, porous ribs in the new design cell are found to play important roles in conditions of excess water: The porous ribs contribute to alleviate water accumulation in the GDL by reserving excess water and increasing the temperature of the GDL especially up on the outlet-side channel.

KEY WORDS: fuel cell, cathode, flow channel, gas diffusion layer, interdigitated, robustness

1. INTRODUCTION

Polymer electrolyte fuel cells (PEFCs) are known as attractive due to their low operating temperature, high energy efficiency (from 40 to 70%) and zero COx and NOx emissions. For further improvement in power density of PEFCs especially for mobility applications, the appropriate design of flow channel is necessary to decrease the voltage loss by the effect of oxygen diffusion resistance in the cathode which is mainly caused by the water accumulation in channels on the separator or in porous structures in the GDL and catalyst layer. We have developed a new gas flow design, which consists of a flat metal separator and a GDL with interdigitated gas-flow channels on its surface, and have found that a single-cell stack with this new design exhibited higher performance than that of a conventional cell in which serpentine or interdigitated channels are formed on the separator[(1),(2)]. Interdigitated flow design is known as its efficient air supply to the catalyst layer caused by the forced convection of the gas in the GDL[(3)]. However, interdigitated flow design is also known that it

has issues on performance stability at high and low humidity conditions. At the high humidity conditions, the nonuniform gas flow occurs as a result of water accumulation in the GDL[4],[5]. At the low humidity, the acceleration of cell dry-out occurs due to forced convection in the GDL.

In the previous study, we constructed cells of 1 × 1 cm active area with the newly designed cell of interdigitated flow channel formed on the GDL and the conventional interdigitated cell with channel formed on the separator, and these performances are compared in various conditions including variations of the relative humidity, the oxygen percentage and the gas flow rate[6]. The experimental results verified the effect of incorporating interdigitated channels in the GDL on alleviating the disadvantages of the conventional interdigitated channels on the separator, particularly under excess water accumulation conditions and dry gas conditions as shown in figure 1. This result indicated that the newly designed cell with interdigitated flow channel on the GDL showed the more stable voltage than the conventional cell with interdigitated flow channel on the separator during high relative humidity of 150% RH, as well, the less degradation of the voltage than the conventional cell under the dry conditions of 15% RH.

We assumed the mechanism of the performance stability in the newly-designed interdigitated cell derives in the existence of the porous ribs. The porous ribs are considered to play different roles in conditions with excess water and dried gas supply for each: In the conditions with excess water, i) the porous ribs contain excess water to alleviate water accumulation in the flat region of the GDL witch interrupt oxygen diffusion to the catalyst layer and ii) the

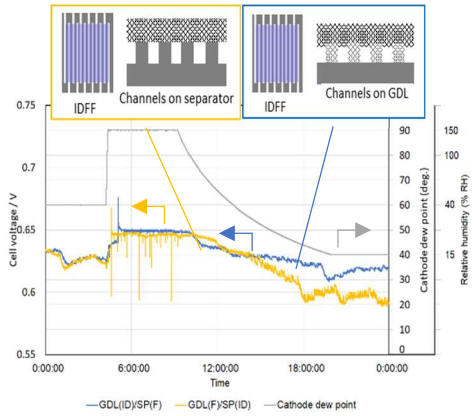

Fig. 1. Changes over time in cell voltages during relative humidity variations from 60% to 150% and 15% RH in a stepwise fashion. The current density was maintained at 1.0 A cm^{-2} during the experiment. The active area of the cell is 1 × 1 cm.

porous ribs increases the temperature in the GDL because of its lower thermal conductivity less than 1/100 compared to solid ribs with graphited carbon or metal material; In the conditions with dried gas supply, iii) accumulated water in the porous ribs gradually diffuse to the flat region of the GDL and compensate the humidity of the catalyst layer and the membrane, and iv) the porous ribs without accumulated water enable some supplied gas to pass through the ribs to alleviate getting rid of remaining water in the flat region of the GDL. To validate predictions from i) to iv), it is desirable to confirm internal phenomenon in the newly designed cell with porous ribs as below for each prediction: i) Water accumulates in the porous ribs in conditions with excess water; ii) The temperature of the flat region of the GDL in the newly designed cell with the porous ribs than in the conventional cell with solid ribs, and is higher than the dew point in the area entirely or partially; iii) The accumulated water in the porous ribs gradually decreases during the operation of the relative humidity decrease; iv) the remaining water in the flat region of the GDL in the newly designed cell are more than that in the conventional cell.

In this study, in order to confirm whether these phenomena above actually occur in the operating cell, we analyzed internal water distribution in the cell under operating conditions by neutron radiography imaging technique. In addition, we calculated the temperature distribution in the GDL by the numerical simulation with three-dimensional model, then compared between the newly designed cell and the conventional cell.

2. NUMERICAL SIMULATION

Hereafter, the symbols of each channel design will be used as defined as follows: GDL with interdigitated ribs + flat separator GDL(ID)/SP(F); and flat GDL + separator with interdigitated ribs, GDL(F)/SP(ID).

To calculate the temperature distribution in the operating cell, Computational Fluid Dynamics (CFD) software package STAR-CCM+ ver. 13.06 was applied by combination with electrochemical solutions. Since it is necessary to simulate the diffusion of both gas flow and liquid flow, Eulerian multiphase mixture model (EMP) was adopted. In EMP, the equation of the energy conservation between two phases, liquid water and vapor in this study, is described as below.

$$\frac{\partial}{\partial t}\int_V \alpha_g \rho_g E_g dV + \oint_A \alpha_g \rho_g H_g \mathbf{v}_g \cdot d\mathbf{a} = \oint_A \alpha_g k_{eff,g} \nabla T_g d\mathbf{a} + \oint_A \mathbf{T}_g \cdot \mathbf{v}_g da + \int_V \mathbf{f}_g \cdot \mathbf{v}_g dV + \int_V \sum_{l \neq g} Q_{gl} dV + \int_V \sum_{(g,l)} Q^{(g,l)} dV + \int_V S_g dV + \int_V \sum_{l \neq g} (m_{gl} - m_{lg}) h_g(T_{gl}) dV \quad (1)$$

List of symbols

A_s	surface area of droplet, m^2
B	Spalding transfer number
C_p	specific heat, J/(kg-K)
D_p	diameter of water droplet, m
E	total energy, eV
E_{eq}^{ox}	equilibrium potential, V
F	Faraday constant, C/mol
f	body force vector, m/s^2
g^*	mass transfer conductance, kg/(m^2-s)
H	total enthalpy, J/kg
h_g (T)	entropy of phase g at T, J/K
i	current density, A/cm^2
i_0	exchange current density, A/cm^2
i_0^{ref}	reference exchange current density, A/cm^2
k	thermal conductivity, J/(s-m-K)
k_{eff}	Effective thermal conductivity, J/(s-m-K)
L	heat of evaporation, J/kg
m_{gl}	mass transfer rate from phase l to phase g, kg/s
$\dot{m}$	mass transfer rate, kg/s
P	pressure, Pa
P_0^{atm}	absolute pressure, Pa
Q_{gl}	amount of transferred heat from phase l to phase g, J/s
$Q_g^{(gl)}$	amount of transferred heat from interface of phase g and phase l to phase g, J/s
R	gas constant, J/(K-mol)
S	energy source term, J/s
T	temperature, K
V	volume, m^3
v	velocity, m/s

Greek

α	volume fraction
α^{eff}	charge transfer coefficient
ρ	density, kg/m^3
μ_t	turbulent viscosity, Pa-s
σ_t	Prandtl number of turbulent heat diffusivity
η	overpotential, V
Φ	potential, V

Subscripts

a	anode
c	cathode
c(g)	vapor
fluid	fluidic regions in fuel cell
g	gas
l	liquid
gl	interface between phase g and phase l
solid	solid regions of fuel cell

Effective thermal conductivity $k_{eff,g}$ is described as below.

$$k_{eff,g} = k_g + \frac{\mu_{t,g} C_{p,g}}{\sigma_{t,g}} \quad (2)$$

Calculation of electrochemical reaction including hydrogen oxidation reaction (HOR) and oxygen reduction reaction (ORR) were based on Butler-Volmer equation.

$$i = i_0 \left[exp\left(\alpha_a^{eff} \frac{F}{RT}\eta\right) - exp\left(-\alpha_c^{eff} \frac{F}{RT}\eta\right)\right] \quad (3)$$

Overvoltage η and exchange current density i_0 are described as below.

$$\eta = -\Phi_{solid} - \Phi_{fluid} - E_{eq}^{ox} \quad (4)$$

$$i_{0,a} = i_{0,a}^{ref} \left(\frac{P_{H2}}{P_0^{atm}}\right)^{0.5} \quad (5)$$

$$i_{0,c(g)} = i_{0,c(g)}^{ref} \left(\frac{P_{O2}}{P_0^{atm}}\right)^{0.5} \left(\frac{P_{H2O}}{P_0^{atm}}\right)^{0.5} \quad (6)$$

Since the evaporation and condensation of water occur in the GDL pores and it brings out thermal production or absorption, Spalding evaporation / condensation model was adopted in MMP to evaluate the effect to the temperature in the GDL. In Spalding model, mass transfer rate $\dot{m}_g$, transference number B and mass transfer conductance g* are described as below.

$$\dot{m}_g = -g^* A_s \ln(1+B) \quad (7)$$

$$B = \frac{C_p(T_g - T_d)}{L} \quad (8)$$

$$g^* = \frac{k_g Nu}{C_{p,g} D_p} \quad (9)$$

From these equations, the temperature at each mesh is calculated as the summation of transferred heat from adjacent meshes, Joule's heat and evaporation or condensation heat at the point.

Figure 2 shows calculation models of GDL(ID)/SP(F) and

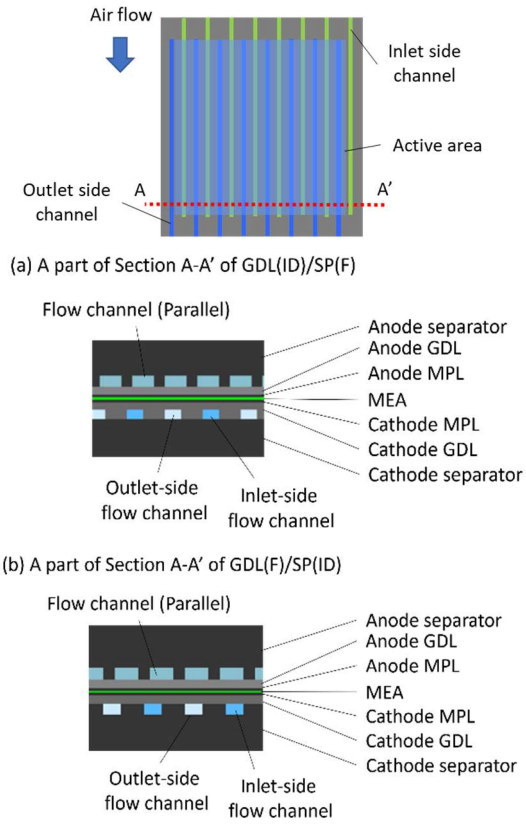

Fig. 2. Schematic images of simulation model. (a): A part of the cross section of A-A' in GDL(ID)/SP(F): (b): A part of the cross section of A-A' in GDL(F)/SP(ID).

GDL(F)/SP(ID). The active area of the model was 1 × 1 cm to repeat the experimental model in our previous study[6]. Parameters of cathode flow channel design and operating conditions are shown in Table 1.

Table 1 Parameters of cathode flow channel design and operating conditions of numerical simulation

Flow channel design	
Channel pitch	0.7 mm (0.4 mm channel width)
Channel depth	0.2 mm
Channel number	16
Operating conditions	
Current density	1.0 A cm^{-2}
Cell temperature	80 °C
Relative humidity	100% RH
Flow rate (Anode/Cathode)	0.5 / 2.0 NL min^{-1}

3. EXPERIMENTS

3.1. Neutron radiography imaging

Since neutron beam has high permeability through cell materials and high sensitivity to water, neutron radiography imaging was brought to measure water distribution in the cell plane quantitively. Neutron radiography was carried out at the beamline BL-22 of Materials and Life Science Experimental Facility (MLF) of Japan Proton Accelerator Research Complex (J-PARC).

Figure 3 shows the structure and the geometry of the experimental cell which was same as our previous study[2]. The active area of the cell was 1.0 × 9.7 cm, and the interdigitated flow channels along the cathode gas flow were divided to three sections. Anode flow channels were serpentine, and the direction of anode gas flow was vertical to the cathode gas flow so that minimize effects on captured neutron images by any difference in structures and materials at the anode.

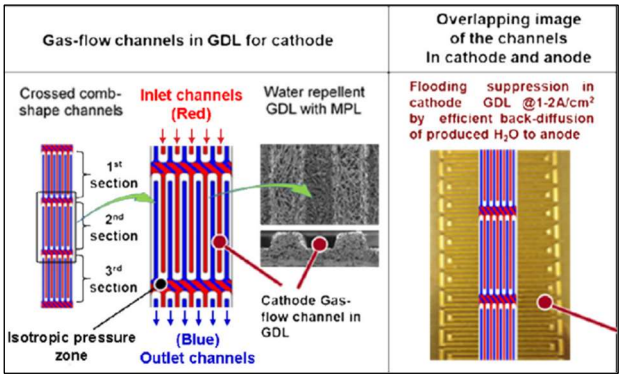

Fig. 3. Structures and the locations of gas flow channels on the GDL applied to the cell for visualization of liquid water by neutron imaging.

Table 2 Operating conditions of the cell for neutron imaging

Current density	3.0 A cm^{-2}
Cell temperature	75 °C
Relative humidity	40% RH
Utilization raio (Hydrogen/Oxygen)	60% / 40% RH

4. RESULTS AND DISCUSSIONS

4.1. Numerical simulation

Figure 5 shows the temperature distribution in the cross section of the GDL and the separator at 1.0 A cm^{-1} current density. In the comparing of (a) GDL(ID)/SP(F) and (b) GDL(F)/SP(ID), the

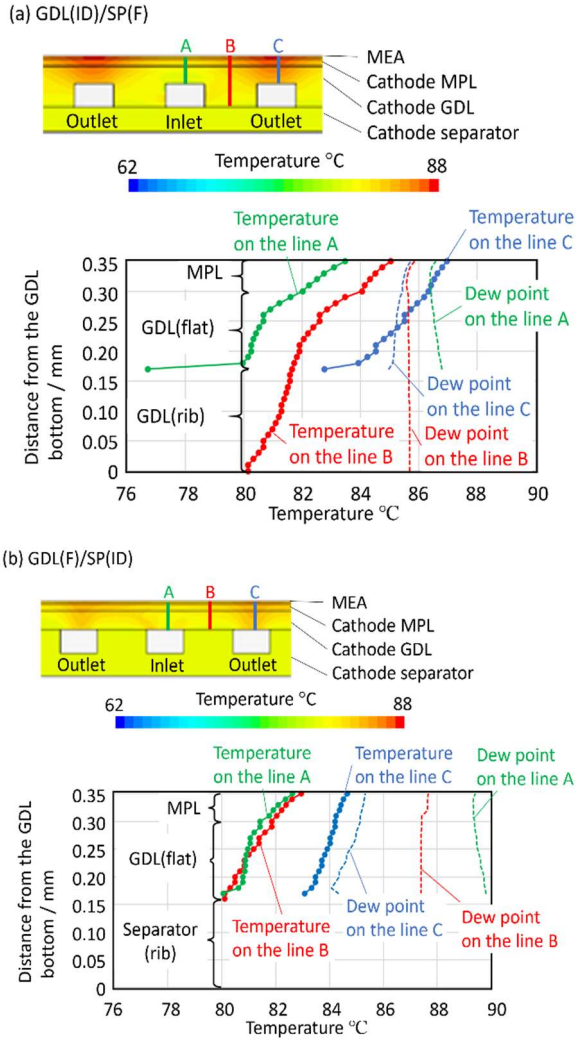

Fig. 4. Temperature distributions in the cross section of (a) GDL(ID)/SP(F) and (b) GDL(F)/SP(ID) obtained by numerical simulations. Line profiles are plots of the temperature distribution along the direction of the GDL width at 3 positions: A is on the inlet side channel; B goes through the rib; and C is on the outlet side channel. Dew points of A, B and C are also plotted to compare with the temperature in the same position.

temperature of the interface between MPL and MEA of GDL(ID)/SP(F) was particularly two degrees Celsius higher than that of GDL(F)/SP(F) at the top of the outlet side channel. From the comparison of the temperature with the dew point at the same position for each, in the case of GDL(ID)/SP(F), the temperature on the outlet side channel (C-C) was higher than the dew point, while that on the other positions were lower. In the case of GDL(F)/SP(ID), the temperature of all positions in the GDL were lower than the dew point.

From these results, as suggested in the proposed mechanism, the temperature of the GDL in GDL(ID)/SP(F) was higher than the dew point on the outlet side channel. This result indicated that water droplet is difficult to remain on the top of the outlet side channel and easily evaporated.

4.2. Neutron radiography imaging

Figure 6 shows the distribution of water thickness in GDL(ID)/SP(F) cell with 1.0 × 9.7 cm active area during operation with 3.0 A cm^{-1} current density. Water thickness was calculated from the attenuation of neutron beam by passing through water in the cell. Figure 6 (B) shows the line profile of the thickness of liquid GDL(ID)/SP(F) cell with 1.0 × 9.7 cm active area during operation with 3.0 A cm^{-1} current density. Water thickness was calculated water on (B-B) crossing upper side of S2 section in figure 6 (A), while figure 6 (C) shows the line profile on (C-C). The blue marker in figure 6 (B) and (C) indicate the position on the outlet channel, while red marker indicates the position on the inlet channel. The gap position of the blue and red marker is the position on the rib. During the distance of from 0.25 to 0.75 cm in figure 6 (C), water thickness on the rib was about 0.05 mm more than that on the inlet and outlet channel. In the case of figure 6 (B), the water thickness on the rib was equivalent to the other position except two positions on the outlet channels saturated with water.

These results indicated the possibility of water accumulation in porous ribs in GDL(ID)/SP(F). Since the porosity of the GDL was about 50% and the height of ribs were 0.18mm, generally half of the vacancy in porous ribs is considered to be occupied with liquid water in down side of the section. Since almost no water accumulation confirmed in porous ribs on upper side of the section in figure 6 (B), liquid water in porous ribs in down side of the section is thought to be the generated water by ORR. From these results and considerations, water accumulation possibly occurred in porous ribs especially in down wide of the stream.

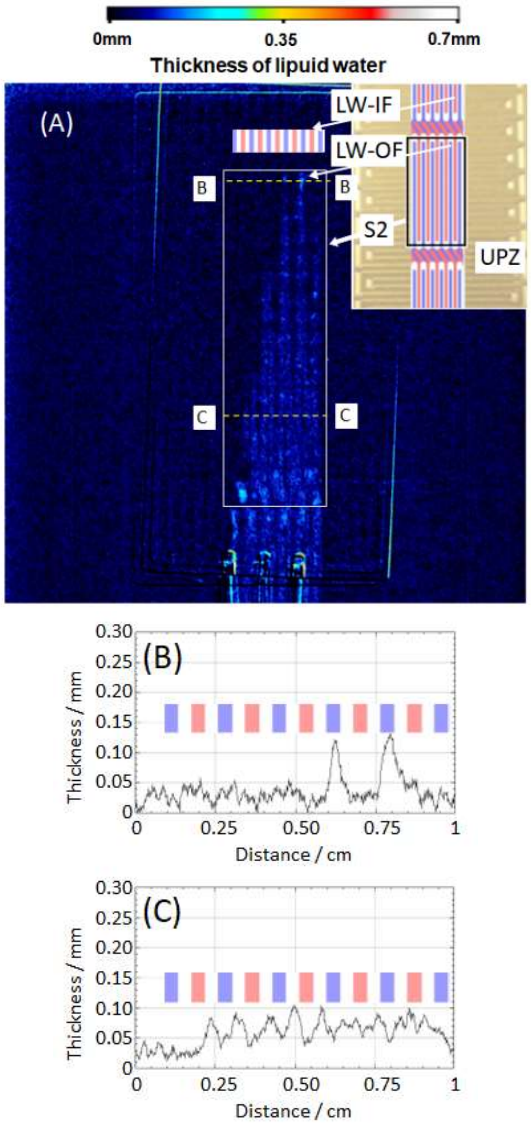

Fig. 5 (A): The image of water distribution in GDL(ID)/SP(F) cell with 1.0 × 9.7 cm active area at 40% RH and 3.0 A cm^{-1} obtained from neutron radiography. S2 indicated the second section of the three. (B): Line profile of the thickness of liquid water on (B-B) crossing upper side of S2 section. (C): Line profile of the thickness of liquid water on (C-C) crossing down side of S2 section.

4.3. Summary of numerical and experimental analysis

To summarize results and considerations, the mechanism of GDL(ID)/SP(F) to increase the performance stability at conditions with excess water was proposed to be as a result of porous ribs existence which plays two innovative roles as below (see figure 6): In operating conditions with high humidity, (i) the supplied liquid water and part of the surplus water generated by ORR in cathode diffuse into porous ribs, thereby the liquid water saturation in the flat region of the GDL can be mitigated. At the same time,

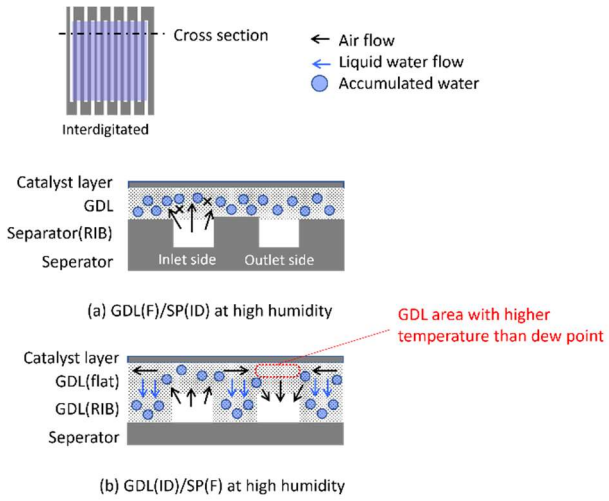

Fig. 6. Schematic illustrations of the mechanism to explain higher cell-performance stability of GDL(ID)/SP(F) by the difference of temperature, gas diffusion and water management at high relative humidity. (a) GDL(F)/SP(ID) and (b) GDL(ID)/SP(F).

(ii) since the ribs are formed by the same material as the GDL, the thermal conductivity of ribs is reduced to 1/100 or less compared to GDL(F)/SP(ID), in which ribs are formed by solid materials such as graphited carbon and metal, the internal temperature of the flat region of the GDL near the interface with the MEA, which is a heat generating point, is higher than that of GDL(F)/SP(ID). Especially the temperature of the flat region of the GDL on the outside channel is higher than the dew point, so the water in the area is difficult to accumulate. These two mechanisms contribute to alleviating the water accumulation in the flat region of the GDL which prevent the oxygen diffusion to the catalyst layer, resulting in the increased performance stability.

5. CONCLUSION

A new gas flow design consisting of a flat metal separator and a GDL with gas-flow channel on its surface was fabricated with interdigitated flow channels and incorporated into single cells. The performance of this newly designed cell was investigated with variations of cell experimental conditions, as a result the newly-designed interdigitated cell with porous ribs was found to increase its performance stability in conditions with excess water compared to the conventional interdigitated cells with solid ribs. To reveal the mechanism of the performance stability in the newly designed cell, numerical simulation based on CFD was applied to clarify the temperature distribution in the GDL and compared between the new and conventional interdigitated cells. As a result of the simulation, the newly-designed cell with interdigitated flow channels on the GDL showed higher temperature at the interface between MPL and MEA than that of the conventional cell with interdigitated flow channels on the separator, especially at the top of the outlet side channel, the temperature of the GDL was higher than the dew point. This result was contributed by the material change of ribs from graphited carbon or metal to porous carbon fiber, and resulting in alleviating water accumulation at the interface between MPL and MEA and improvement of the performance stability. In addition, to visualize water distribution in the newly designed cell under the operation, neutron radiography imaging technique are applied. The result of neutron image showed the possibility of liquid water existence in the porous ribs, especially in the down side of the stream. As results of these studies, interdigitated porous ribs were found to play important and functional roles: in conditions of excess water, porous ribs contribute to alleviate water accumulation in the GDL by reserving excess water and increasing the temperature of the GDL up on the outlet-side channel.

ACKNOWLEDGMENT

This work was partially supported by the “Fuel Cells–Yamanashi Frontier for Innovation and Ecosystem (FCyFINE)” program (2017–2021), supported by the Ministry of Education, Culture, Sports, Science and Technology, Japan, and was partially supported by funds for the “Electrolytes, catalysts and catalyst layers with extraordinary efficiency, power and durability for PEFCs to 2030” (ECCEED-GDL) project from the New Energy and Industrial Technology Development Organization (NEDO). The neutron experiments were conducted at MFL of J-PARC.

REFERENCES

(1) M. Watanabe, H. Yanai and M. Nasu, Journal of The Electrochemical Society, 166, 3210 (2019).

(2) M. Nasu, H. Yanai, N. Hirayama, H. Adachi, Y. Kakizawa, Y. Shirase, H. Nishiyama, T. Kawamoto, J. Inukai, T. Shinohara, H. Hayashida and M. Watanabe, Journal of Power Sources, 530, 231251 (2022).

(3) T. V. Nguyen, J. Electrochem. Soc., Vol. 143, No.5 (1996).

(4) A. D. Le and B. Zhou, Journal of Power Sources, 193, 665, (2009).

(5) T. V. Nguyen and M. W. Knobbe, Journal of Power Sources, 114, 70 (2003).

(6) T. Inoue, D. Sakai, K. Hirota, K. Sano, M. Nasu, H. Yanai, M. Watanabe, A. Iiyama and M. Uchida, Journal of The Electrochamical Society, Vol. 169, No. 11(2022)